Total Variation Compressive Sensing for Extended Targets in MIMO Radar

Roldan, Ignacio; Fioranelli, Francesco; Yarovoy, Alexander

DOI
10.1109/SAM53842.2022.9827822

Publication date
2022

Document Version
Final published version

Published in
2022 IEEE 12th Sensor Array and Multichannel Signal Processing Workshop, SAM 2022

Total Variation Compressive Sensing for Extended Targets in MIMO Radar

Ignacio Roldan
MS3, Department of Microelectronics
TU Delft
Delft, The Netherlands
i.roldanmontero@tudelft.nl

Francesco Fioranelli
MS3, Department of Microelectronics
TU Delft
Delft, The Netherlands
f.fioranelli@tudelft.nl

Alexander Yarovoy
MS3, Department of Microelectronics
TU Delft
Delft, The Netherlands
a.yarovoy@tudelft.nl

2022 IEEE 12th Sensor Array and Multichannel Signal Processing Workshop (SAM) | 978-1-6654-0633-8/22/$31.00 ©2022 IEEE | DOI: 10.1109/SAM53842.2022.9827822

***Abstract*—The problem of extended target cross-section estimation has been considered. A two-step method based on the Total Variation Compressive Sensing theory has been proposed to solve it. First, a coarse estimation of the target cross-section is performed with classical beamforming methods, and then Compressive Sensing algorithms have been applied to refine it. To the best of the authors' knowledge, this is the first time this approach has been applied to automotive radar signals. The method has been verified simulating extended targets as scatter point clouds and computing the response in a uniform rectangular array. Two metrics have been used, the Intersection over Union and a pseudo Integrated Sidelobe Level. Significant improvements in both metrics compared with classical beamforming methods have been demonstrated.**

***Index Terms*—Compressive Sensing, Total Variation Normalization, MIMO automotive radar, Extended Targets**

I. Introduction

Automotive radar is key for advanced driver assistance systems (ADAS), thanks to its high reliability in measuring range, speed, and direction of arrival (DoA) in challenging, low-visibility environmental conditions when cameras and lidar fail. In the early days of automotive radars, only range and speed were measured; however, the current state-of-the-art is transitioning into 4D imaging radars, measuring azimuth and elevation angles as well [1]–[3]. This 4D imaging radar technology aims to deliver image-like fine resolution point clouds, approaching the performance of lidar systems but at a lower cost. With this improved resolution, the size of the observed objects is larger than the resolution cell, and thus objects are extended into multiple resolution cells. To deal with this phenomenon and accurately estimate the DoA and the extent of the targets, new algorithms must be developed.

Automotive radars are based on multiple-input multiple-output (MIMO) architecture, which uses a different array of transmitting and receiving antennas to form a virtual array with higher spatial diversity. Different super-resolution algorithms, such as multiple signal classification (MUSIC), minimum variance distortionless response (MVDR), or estimation of signal parameters via rotational invariance techniques (ESPRIT), have been widely exploited to estimate the DoA of the signals in MIMO radars. However, all these algorithms are unsuitable for new-generation imaging radars [4]. First, they require an accurate estimation of the number of targets before their application, assuming uncorrelated sources. This estimation works well only when a few targets are present and they behave as single scatter points (i.e., their size is smaller than the resolution cell). For high-resolution radar imaging, a single target behaves like a cloud of scatterers, and thus the estimation of the number of sources will not be reliable. Secondly, the computational complexity of such methods increases with the number of detected targets, which will grow as the resolution increases. Finally, these algorithms only work with conventional dense arrays with no more than half wavelength separation between antennas, and thus are unsuitable for sparse arrays.

This work presents a method based on the compressive sensing (CS) theory for estimating simultaneously the azimuth and elevation angles of extended targets. The method uses a two-step algorithm, where first a coarse estimation for the whole scene with classical beamforming is performed, and then it is locally refined with the CS estimation. Moreover, a total variation regularization is used, which allows an accurate reconstruction of the target's shape.

The rest of the paper is organized as follows. Section II introduces the signal model of a 2D MIMO array and formulates the problem. In Section III, the proposed two-step algorithm for 2D angular reconstruction is presented in detail. The performance evaluation on simulated targets is presented in Section IV. Finally, conclusions are drawn in Section V.

II. Problem Formulation

The conventional spherical coordinate systems is considered, with azimuth angle denoted by θ and elevation angle by ϕ. The MIMO radar is located in the xz plane, with the transmitter and receiver arrays closely located, so that targets in the far-field are at the same distance from both arrays. The transmitted waveforms are assumed to be mutually orthogonal, and the individual elements are isotropic antennas for the $y > 0$ half-space. An arbitrary topology array is considered, where $\mathrm{N_t}$ is the number of elements in the transmitter array, and $\mathrm{N_r}$ is the number of elements in the receiver array. For a far-field point, the steering vectors of the transmitter and receiver array can be described as:

$$a(\theta^{'},\phi^{'}) = \begin{pmatrix} e^{-j\frac{2\pi}{\lambda}(x_{t,1}\cos\theta^{'}\sin\phi^{'}+z_{t,1}\cos\phi^{'})} \\ \cdot \\ \cdot \\ e^{-j\frac{2\pi}{\lambda}(x_{t,N_t}\cos\theta^{'}\sin\phi^{'}+z_{t,N_t}\cos\phi^{'})} \end{pmatrix}, \quad (1)$$

$$b(\theta^{'},\phi^{'}) = \begin{pmatrix} e^{-j\frac{2\pi}{\lambda}(x_{r,1}\cos\theta^{'}\sin\phi^{'}+z_{r,1}\cos\phi^{'})} \\ \cdot \\ \cdot \\ e^{-j\frac{2\pi}{\lambda}(x_{r,N_r}\cos\theta^{'}\sin\phi^{'}+z_{r,N_r}\cos\phi^{'})} \end{pmatrix}, \quad (2)$$

where x_t, z_t, x_r, z_r are the coordinates of the arrays' elements, and λ is the wavelength. With orthogonal transmitted waveforms, a new virtual array of $\mathrm{N_t N_r}$ elements can be formed. Its steering vector is given by the Kronecker product of the transmitter and receiver steering vectors, as:

$$v(\theta^{'},\phi^{'}) = a(\theta^{'},\phi^{'}) \otimes b(\theta^{'},\phi^{'}) = \begin{pmatrix} e^{-j\frac{2\pi}{\lambda}((x_{t,1}+x_{r,1})\cos\theta^{'}\sin\phi^{'}+(z_{t,1}+z_{r,1})\cos\phi^{'})} \\ \cdot \\ \cdot \\ e^{-j\frac{2\pi}{\lambda}((x_{r,N_t}+x_{r,N_r})\cos\theta^{'}\sin\phi^{'}+(z_{r,N_t}+z_{r,N_r})\cos\phi^{'})} \end{pmatrix} \quad (3)$$

This paper aims to estimate the DoA angles of extended targets, and therefore, the time delay due to target range and Doppler shift are not shown in the model. This is justified by the fact that angular resolution is independent of range and Doppler resolution in MIMO radars [5]. Thus, the received single snapshot baseband signal (i.e., only one chirp transmitted per transmitter) can be written in matrix form as:

$$y = \tilde{\boldsymbol{A}}(\theta,\phi)\tilde{x} + e, \quad (4)$$

where $y \in \mathbb{C}^{N_r N_t \times 1}$ is the complex sample vector, $e \in \mathbb{C}^{N_r N_t \times 1}$ is the additive complex Gaussian noise, and $\tilde{\boldsymbol{A}} \in \mathbb{C}^{N_r N_t \times K}$ is the measurement matrix formed by the virtual steering vectors pointing to K targets as:

$$\tilde{\boldsymbol{A}}(\theta,\phi) = [v(\theta_1,\phi_1), ..., v(\theta_K,\phi_K)] \quad (5)$$

From a classical signal processing point of view, $\tilde{\boldsymbol{A}}$ and $\tilde{x}$ are unknowns, and the goal is to estimate them using y. However, this problem can be cast as a CS problem by discretizing the azimuth-elevation space in a grid of M points, and assuming the targets locations lie on this grid. A new dictionary matrix $\boldsymbol{A} \in \mathbb{C}^{N_r N_t \times M}$ can be constructed where each steering vector points to the grid points, and thus, the received signal can be expressed as:

$$y = \boldsymbol{A}x + e, \quad (6)$$

where $x \in \mathbb{C}^{M \times 1}$ is an unknown vector containing the reflected power of the targets and encoding their angular position. Note that the $\boldsymbol{A}$ matrix is known in this case, pre-computed a-priori by stacking virtual steering vectors.

In the standard CS framework, the undetermined system of equations in (6) is solved by enforcing sparsity in the signal x (i.e., $M \gg G$, and thus x contains only a few non-zero elements) via the $l1$-norm minimization problem given by:

$$\min_x ||x||_1 \quad s.t. \quad \boldsymbol{A}x = y \quad (7)$$

Many studies have successfully solved the optimization problem given by (7) in the radar field [6], [7]. However, if large extended targets are present in the scene, the signal may not be sparse enough in the DoA domain, and the recovery guarantees given by the restricted isometry property (RIP) may not hold. For this reason, an alternative approach is proposed in this paper using the total variation compressive sensing (TVCS) framework. In this framework, instead of assuming the signal is sparse, the assumption is that the gradient of the signal is sparse. The TVCS minimization problem given in (8) aims to find the signal whose gradient is the sparsest, thus preserving the edges or boundaries more accurately. This model is more appropriate for large extended targets because only a few sharp transitions are present in the DoA domain, i.e., at the edges of the object, and thus the gradient is sparse. The recovery guarantees of the TVCS are discussed in [8].

$$\min_x ||\nabla x||_1 \quad s.t. \quad \boldsymbol{A}x = y \quad (8)$$

However, the formulation given in (8) has two main problems: it is hard to solve because it is non-differentiable and non-linear, and solving it might be too computationally complex. In the next section, these two issues will be addressed.

III. Proposed Method

The proposed method uses a two-step process to reduce computational complexity. First, classical delay and sum (DS) beamformer [9] is applied to estimate the approximate location of the objects. Then, the $\boldsymbol{A}$ matrix is dynamically built with steering vectors pointing only to the local regions where the potential targets are. With this, the dimensionality of $\boldsymbol{A}$ is drastically reduced. Now, for the reduced version of $\boldsymbol{A}$, (8) must be solved. Different methods have been proposed in the literature to solve this problem, but in this work the TV minimization by augmented lagrangian and alternating direction algorithm (TVAL3) [10] is used because of its efficiency [11]. The first step of TVAL3 is to reformulate (8) into an equivalent form introducing a set of auxiliary variables as:

$$\min_{w,x} ||w||_1 \quad s.t. \quad \boldsymbol{A}x = y \text{ and } \nabla x = w \quad (9)$$

Then, to cast the problem into a sequence of unconstrained optimization problems, the well-known augmented Lagrangian is used as:

$$\begin{aligned}\mathcal{L}(w,x) =& ||w||_1 - v^T(\nabla x - w) + \frac{\beta}{2}||\nabla x - w||_2^2 \\ & - r^T(\boldsymbol{A}x - y) + \frac{\mu}{2}||\boldsymbol{A}x - y||_2^2,\end{aligned} \quad (10)$$

where $.^T$ is the transpose operator, $||.||_2$ is the $l2$-norm, β and μ are the penalty terms, and v and r are the Lagrangian multipliers. Therefore, (9) can be reformulated as:

$$\min_{w,x} \mathcal{L}(w, x) \tag{11}$$

Finally, this unconstrained optimization problem series is solved using the alternating direction method proposed in [10]. In several fields, TVAL3 has been proved to be one of the most efficient total variation regularization solvers [12], [13], and combined with the dimensionality reduction of $\boldsymbol{A}$, the computational time is reduced significantly. The following section provides some examples of DoA estimation for extended targets using this two-step approach.

IV. Numerical Results

This section presents numerical results to assess the proposed method's performance. First, several extended targets with different shapes have been simulated as a cloud of scatter points with the same radar cross section (RCS). Examples of these targets can be seen on the leftmost two plots of Fig. 1. The scatter points have been spaced 1° in both azimuth and elevation and have been randomly shifted by ±0.25° to avoid the so-called 'inversion crime' (i.e., the points lie precisely in the discretized grid). Also, it can be seen in black dotted line the convex haul, which will be used as the target boundary.

Then, a 20Tx-20Rx MIMO radar system that yields a 20×20 virtual uniform rectangular array (URA) with $\lambda/2$ separation between elements is simulated. The signal reflected by each scatter point is computed and aggregated in each virtual element to generate the y sample vector. After reshaping, a conventional DS beamformer can be applied to perform the azimuth-elevation estimation. An example of this beamforming with a zoom in the region of interest can be seen in the sub-figures in the second column of Fig. 1. Then, the reduced version of $\boldsymbol{A}$ is computed in a 1° grid within the zoomed area, and optimization problem (11) is solved. The result yielded by the TVAL3 algorithm can be seen in the rightmost column of Fig. 1. The default TVAL3 parameters proposed by the authors have been used, except μ, which has been lowered to 2^4 to guarantee a good performance in the cases with a high noise level. By visual inspection, it is clear that the reconstruction using TVAL3 represents better the shape of the targets, as well as having lower sidelobes. These two aspects are the key metrics to assess the algorithm's performance.

In order to evaluate the similarity between the real shape and the reconstructed shape of the target, a shape must be extracted from the azimuth-elevation matrix. In this paper, the boundary at the -10dB drop from the maximum value in each image has been chosen to define the reconstructed shape. It is not in the scope of the article to discuss an appropriate value for this definition of the shape, and changing this -10 dB threshold does not change the results from a qualitative point of view. An example of these boundaries can be seen as the dotted black line in the middle and rightmost columns of Fig. 1. Moreover, Fig. 2 shows an example of the real and

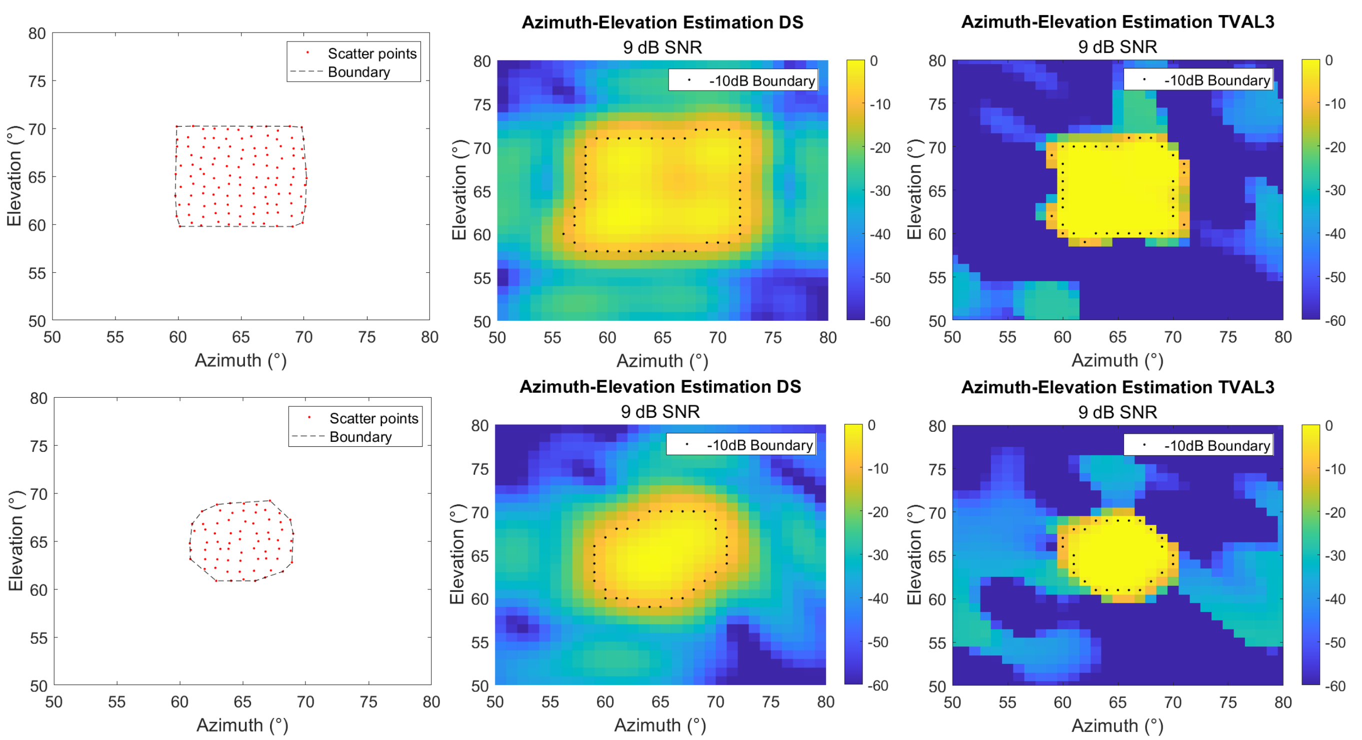

Fig. 1. On the leftmost column, the cloud scatter points simulate distributed targets. In the middle, the reconstructed azimuth-elevation matrix using a conventional DS beamformer. On the rightmost column the output of the TVAL3 algorithm is shown. The simulations assumed 9dB of SNR.

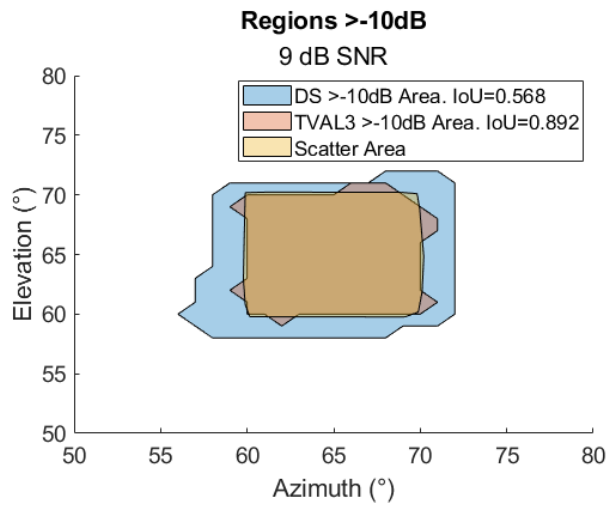

Fig. 2. Original and reconstructed shapes using a DS beamformer and TVAL3. In this case, a rectangular target has been simulated. It can be seen how the TVAL3 reconstructs the target's shape better, yielding an IoU of 0.886.

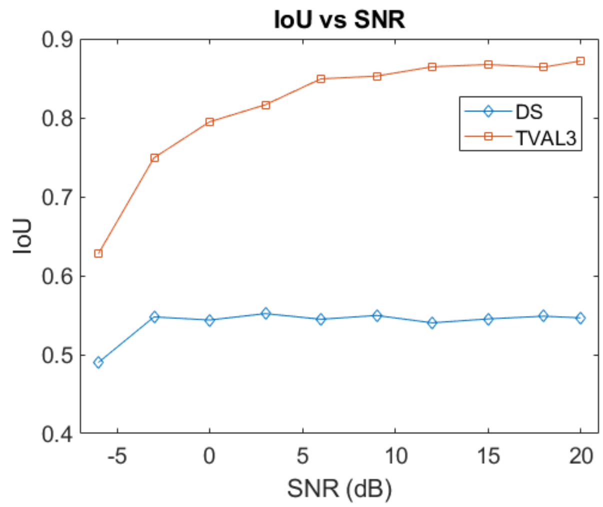

Fig. 3. IoU vs SNR for different targets' shape and locations.

reconstructed shapes as colored areas, for one realization of a rectangular target. Once the target shape has been determined given the aforementioned threshold, the Jaccard index, also named intersection over union (IoU), is computed between the real and estimated shape. The IoU metric is equal to 1 when two areas perfectly overlap and goes to 0 when there is no union between them. A Monte Carlo simulation has been implemented, modifying the target shape, position, and signal to noise ratio (SNR). 100 trials have been simulated with three shapes: rectangular, triangular and circular. The position of the targets has been uniformly sampled in ±60° for both angles. The results aggregated for each SNR are presented in Fig. 3. It is important to note that the SNR refers to the ratio before the angular processing, i.e., before the DS gain or TVAL3 gain. It can be seen how the IoU is higher in the TVAL3 case for every SNR and only start decaying for rather low values. This appears to indicate that it is a robust method against noise.

However, the IoU metric only provides an indication of how well the shape is reconstructed, but does not consider how the energy is spread into secondary lobes. This is not only important because of its influence on the reconstruction quality, but also could prevent weak targets detection. For this reason, a pseudo integrated side lobe level ratio (P-ISLR) is computed, where all the energy inside the real target boundary is considered as the main lobe, and all the energy outside is considered as sidelobes. Again, this test is repeated in a Monte Carlo fashion for different target shapes and locations. The results for different SNRs are shown in Fig. 3. It can be seen how the TVAL3 reconstruction outperforms significantly in terms of P-ISLR.

V. Conclusions

A Compressive Sensing based method to estimate the cross-section of extended targets using MIMO radars is presented in this paper. It is based on the Total Variation regularization to enforce sparsity in the signal's gradient, preserving the edges of the targets. The TVAL3 algorithm has been used for its high efficiency, which solves the CS optimization problem using the alternating direction method. Different extended objects have been simulated with different shapes, and the algorithm has been applied to the signal collected with a 20×20 URA system. To assess the performance, results have been compared with the reconstruction obtained using a classical DS beamformer for two key metrics. First, the IoU of the real and reconstructed shapes have been computed to assess the accuracy of the shape reonstruction, for which TVAL3 clearly outperforms the classical beamforming. Then, the P-ISLR has been computed to evaluate the impact of the algorithm in the sidelobe level, critical for detecting weak targets near strong reflectors (i.e., a pedestrian next to a truck). Again, the TVAL3 reconstruction performs well, even in low SNR scenarios.

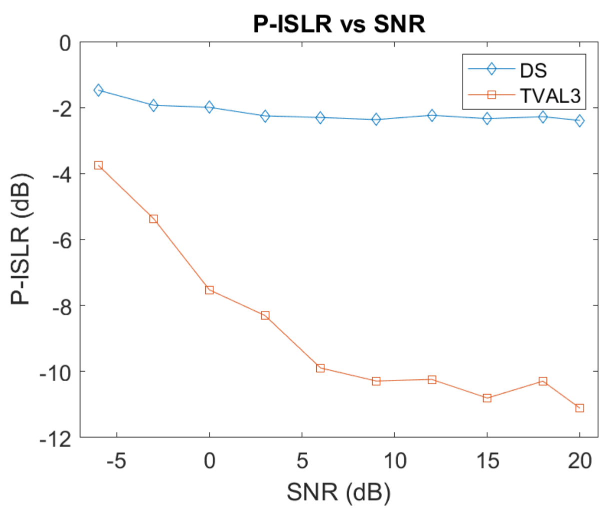

Fig. 4. P-ISLR vs SNR for different targets' shape and locations.

REFERENCES

[1] S. M. Patole, M. Torlak, D. Wang, and M. Ali, "Automotive radars: A review of signal processing techniques," *IEEE Signal Processing Magazine*, vol. 34, pp. 22–35, 3 2017.

[2] G. Hakobyan and B. Yang, "High-performance automotive radar: A review of signal processing algorithms and modulation schemes," *IEEE Signal Processing Magazine*, vol. 36, pp. 32–44, 9 2019.

[3] F. Engels, P. Heidenreich, M. Wintermantel, L. Stacker, M. Al Kadi, and A. M. Zoubir, "Automotive Radars Signal Processing: Research Directions and Practical Challenges," *IEEE Journal on Selected Topics in Signal Processing*, vol. 15, no. 4, pp. 865–878, 2021.

[4] S. Sun, A. P. Petropulu, and H. V. Poor, "MIMO Radar for Advanced Driver-Assistance Systems and Autonomous Driving: Advantages and Challenges," *IEEE Signal Processing Magazine*, vol. 37, no. 4, pp. 98–117, jul 2020.

[5] J. V. DiFranco and W. L. Rubin, "Spatial ambiguity and resolution for array antenna systems," *IEEE Transactions on Military Electronics*, vol. 9, no. 3, pp. 229–237, 1965.

[6] M. Rossi, A. M. Haimovich, and Y. C. Eldar, "Spatial compressive sensing for mimo radar," *IEEE Transactions on Signal Processing*, vol. 62, no. 2, pp. 419–430, 2014.

[7] Y. Yu, A. P. Petropulu, and H. V. Poor, "Mimo radar using compressive sampling," *IEEE Journal of Selected Topics in Signal Processing*, vol. 4, no. 1, pp. 146–163, 2010.

[8] F. Krahmer, C. Kruschel, and M. Sandbichler, "Total variation minimization in compressed sensing," *CoRR*, vol. abs/1704.02105, 2017.

[9] H. L. Van Trees, *Optimum array processing*. John Wiley & Sons, 2002.

[10] C. Li, W. Yin, and Y. Zhang, "Tval3: Tv minimization by augmented lagrangian and alternating direction algorithm," 2009. [Online]. Available: https://www.caam.rice.edu/ optimization/L1/TVAL3/

[11] C. Li, W. Yin, H. Jiang, and Y. Zhang, "An efficient augmented lagrangian method with applications to total variation minimization," *Computational Optimization and Applications*, vol. 56, no. 3, pp. 507–530, Dec 2013.

[12] Q. Kong, R. Gong, J. Liu, and X. Shao, "Investigation on reconstruction for frequency domain photoacoustic imaging via tval3 regularization algorithm," *IEEE Photonics Journal*, vol. 10, no. 5, pp. 1–15, 2018.

[13] X. Liu, L. Zhang, Y. Zhang, and L. Qiao, "A comparative study of four total variational regularization reconstruction algorithms for sparse-view photoacoustic imaging," *Computational and Mathematical Methods in Medicine*, vol. 8, pp. 1046–1055, Oct 2021.